

## MICRO CATALYTIC COMBUSTOR WITH TAILORED Pt/Al<sub>2</sub>O<sub>3</sub> FILMS

Yuji SUZUKI, Yuya HORII, and Nobuhide KASAGI

Department of Mechanical Engineering, the University of Tokyo

7-3-1, Hongo, Bunkyo-ku, Tokyo 113-8656, JAPAN

e-mail: ysuzuki@thtlab.t.u-tokyo.ac.jp, Tel.: +81-3-5841-6411

Micro catalytic combustion of butane in microtube is investigated. Porous alumina fabricated on the inner surface of microtube through anodic oxidation of Al is employed for the support of Pt catalyst. Exhaust gas is sampled to measure its composition and the combustion efficiency. Combustion starts at 250 °C, and a heat release rate up to 250MW/m<sup>3</sup> is achieved in a 0.6mm ID tube. A silicon-based catalytic combustor is designed and its prototype is fabricated using MEMS technologies. The Pt/alumina catalyst layer is successfully integrated onto a silicon microchannel, and a Pyrex lid is anodically bonded onto the Si substrate. It is found in a preliminary experiment that the MEMS combustor also works well, but gives somewhat smaller reaction rate due to the thinner catalytic layer.

**Key Words:** Catalytic combustor, anodic oxidation, Pt/Al<sub>2</sub>O<sub>3</sub> catalyst, MEMS

### INTRODUCTION

Due to recent advances of mobile electronic devices such as laptop computer and cellular phone, the worldwide demand for primary and secondary batteries is growing annually and projected to be \$59 billion in 2006[1]. Li-ion battery has the highest energy density among secondary batteries for consumer use, but its energy density is projected to reach only 300Wh/kg. On the other hand, the energy density of hydrocarbon fuel such as methanol and butane is up to two orders of magnitudes larger. Therefore, local power generation having only a few percent conversion efficiency can provide much higher energy density than Li-ion batteries.

Recently, MEMS gas turbine[2], micro rotary IC engine[3], micro fuel cell[4], and micro thermoelectric power generator[5] are proposed for portable power generation systems. However, each system has its own challenges or drawbacks as well as advantages. Therefore, no single system is currently considered to prevail the others in real applications.

Final goal of the present study is to develop an external combustion engine such as micro steam engine or micro stirling engine[6]. In these systems, combustion in small scale is one of the most important technological issues. For hydrocarbon fuels, reaction speed is much slower than hydrogen and quenching should occur in sub-millimeter scale. Therefore, heterogenous catalytic combustion rather than homogeneous gas phase reaction is preferred[7-11].

The objectives of the present study are to develop micro catalytic combustor with anodized alumina support and to evaluate its performance in a series of laboratory experiments.

### CATALYST LAYER

In the present study, catalyst support layer is made through anodic oxidation of aluminum film deposited on the substrate using thermal evaporation. The advantages of the anodized alumina support are three folds; firstly, unlike solgel methods, it is easy to control the support thickness and its characteristics such as porosity. Secondary, adhesion between alumina and aluminum is good, so that the catalyst layer is robust for thermal shock expected to occur for micro combustors. Thirdly, once aluminum layer is formed, it is easy to change it into alumina through anodic oxidation even for complex geometries.

Figure 1 shows the fabrication process of Pt/alumina catalyst. Anodic oxidation is made using 4 wt% oxalic acid solution. The temperature of the solution is kept constant at 10 °C using an external water loop. A constant current source and a stainless steel plate are respectively employed for the power supply and the cathode. After the oxidation followed by a bake at 350 °C for 1 hour, porous alumina ( $\gamma$ -Al<sub>2</sub>O<sub>3</sub>) is formed on the anode surface. Then, the sample is submerged into diammine dinitro platinum (II) solution, and calcinated at 350 °C for 1 hour to make platinum impregnated into the alumina layer.

Figure 2 shows SEM images of the alumina layer anodized with current density  $I_A$  of  $50\text{A/m}^2$ . Honeycomb-like pore structures can be seen, although the pore diameter and the distance between pores are not uniformly distributed. The pore characteristics of the alumina and its thickness depend on the current density and the oxidation duration [12,13]. In the present study,  $5\mu\text{m}$ -thick alumina is obtained with 1 hour anodization. Diameter of the pore is about  $20\text{-}30\text{nm}$ , which is in agreement with the result of Sungkono et al. [13]. Distance between neighboring nanopores is about  $90\text{nm}$ , which corresponds to the surface area of  $2\text{ m}^2/\text{g}$ . After impregnation of Pt, the catalyst layer is examined with X-ray fluorescent analysis in order to confirm presence of Pt. Contents of Pt in the alumina layer is designed to be around 1 wt%, although it is not directly measured in the present study.

### COMBUSTION EXPERIMENT IN MICRO TUBE

In our first stage, catalytic layer is formed inside aluminum tube of which inner diameter is  $D=0.6\text{mm}$  and the combustion characteristic is measured systematically. The outer diameter and the length of the tube is respectively  $1\text{mm}$  and  $50\text{ mm}$ .

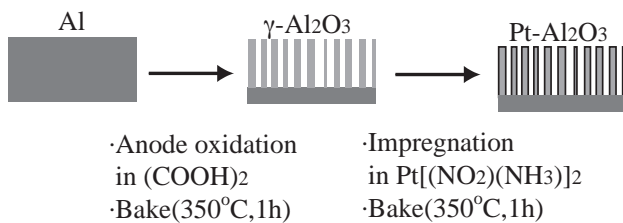


Figure 1 Fabrication process for Pt/  $\text{Al}_2\text{O}_3$  catalyst.

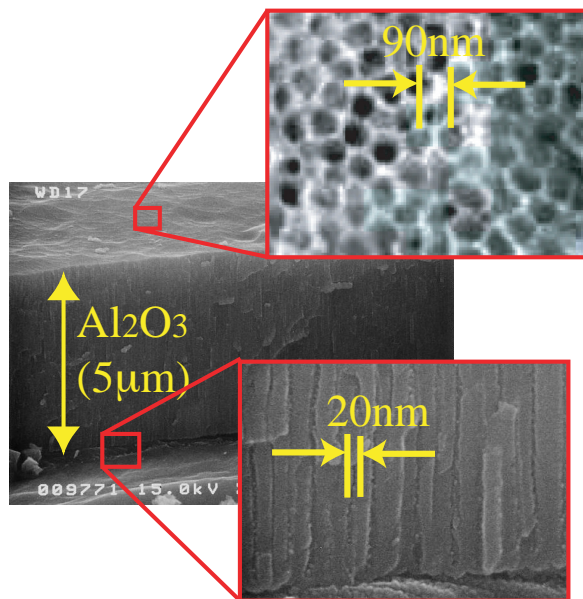
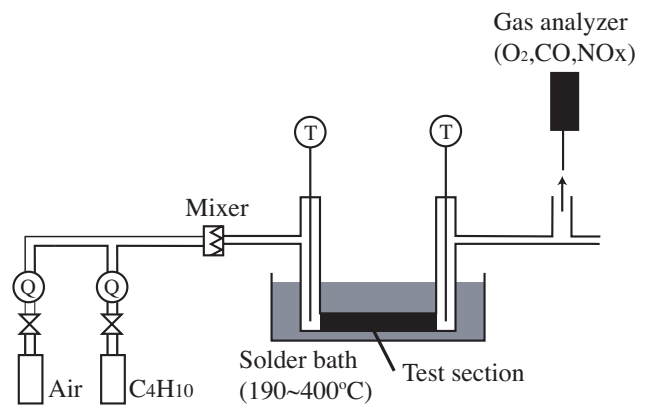


Figure 2 SEM images of  $\text{Al}_2\text{O}_3$  layer made by anodic oxidation at  $I_A=50\text{A/m}^2$  for 1h.

Figure 3 shows a schematic of the present experimental setup. Air and  $n$ -butane are supplied from a gas cylinder and introduced into a mixer. Flow rate is separately measured using thermal mass flow meters (Oval Corp., MASFLO). Combustion experiment is made in a solder bath, by which the solder temperature can be maintained between  $190$  and  $400\text{ }^\circ\text{C}$ . Due to high thermal conductivity and large heat capacity of the solder, temperature of the combustion tube can be kept constant almost independently of the amount of heat generation in the combustion tube. Actual temperature of the catalytic layer is estimated with the inlet and outlet gas temperature assuming that the heat transfer coefficient at the tube inner wall can be given by its theoretical value of the fully-developed laminar forced convection.

Exhaust gas analyzer (TSI Inc., CA-6215) is employed to measure concentration of  $\text{O}_2$ ,  $\text{CO}_2$  and  $\text{NO}_x$ . The reaction rate is calculated using the  $\text{O}_2$  concentration at the exit. In the present experiment condition, the equivalent ratio is kept unity and the flow rate of  $n$ -butane is changed between  $2.5 - 25\text{ sccm}$ , which correspond to the heat generation at 100% conversion  $Q$  of  $5 - 50\text{ W}$ . The Reynolds number is less than 160 in all the experimental condition examined. Therefore, velocity and thermal entrance lengths are less than  $8D$ , and their effect is believed to be minor.

Figure 4 shows reaction heat in the combustion tube anodized with  $I_A=50\text{A/m}^2$  for 12 hours. Thickness of the alumina is estimated to be  $35\mu\text{m}$ . Onset of combustion starts around  $250\text{ }^\circ\text{C}$  and the heat generated is increased with the catalyst temperature. At  $400\text{ }^\circ\text{C}$ , 100% conversion is achieved up to  $Q=10\text{W}$ , while the maximum heat generation is  $32\text{W}$  at  $450\text{ }^\circ\text{C}$  for  $Q=50\text{W}$ . Therefore, heat generation density for 100% conversion is as large as  $250\text{ MW/m}^3$ , which is comparable to that of the industrial gas turbine combustors. In macro scale catalyst combustors, dif-



Q: Volumetric flow meter

$T_1, T_2$ : Thermocouple

Figure 3 Experimental setup.

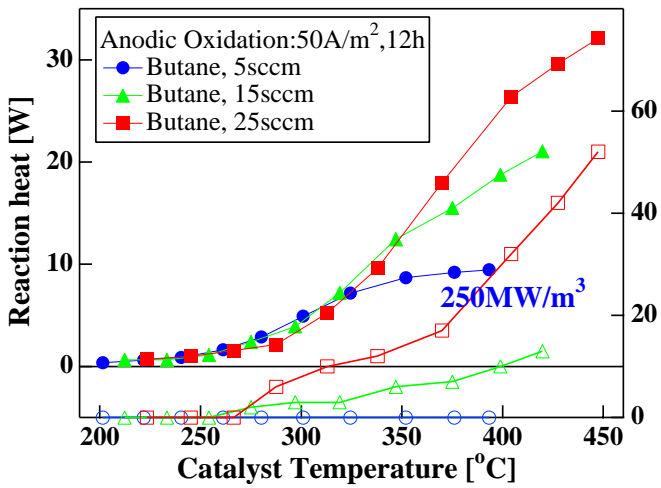


Figure 4 Reaction heat and exhaust CO concentration in 0.6mm ID combustor tube with Pt/Al<sub>2</sub>O<sub>3</sub> catalyst .

fusion in the bulk fluid is the major limiting factor, and the heat generation density is generally lower than homogenous well-stirred combustors. On the other hand, in micro combustors having a small hydraulic diameter, diffusion in fluid is no more the limiting factor, and diffusion in the catalyst layer and the reaction speed itself should play a dominant role in determining the overall reaction rate.

As also shown in Fig. 4, concentration of CO is almost zero for  $Q=10W$ . But, it becomes finite value when  $Q$  is larger than 10W. Note that NO<sub>x</sub> concentration is always less than 1 ppm and within the measurement accuracy of the gas analyzer.

### MEMS CATALYTIC COMBUSTOR

Figure 5 shows a schematic of Si-based catalytic combustor. Trapezoidal channels are etched into the Si substrate. The surface area of the Pt/alumina catalytic layer is chosen as the same as that of the 0.6mm ID tube shown in the previous chapter. Hydraulic diameter of each channel is 261μm.

Fabrication process (Fig. 6) starts with patterning the SiO<sub>2</sub> layer on a (100) Si wafer for the channel and the fluid ports followed by an anisotropic etching with TMAH. The oxide mask layer is removed with BHF and a 1μm-thick 2nd oxide layer is formed using wet oxidation for an electrical insulation layer. Aluminum film is then evaporated and patterned in such a way that aluminum remains only inside the channel. The aluminum film is transformed into alumina using anodic oxidation as described above. Finally, Pyrex glass wafer is anodically bonded to the Si wafer and Pt catalyst is impregnated.

Figure 7 shows a top view of the Si-based catalytic combustor having 8 parallel channels and two fluidic ports. The

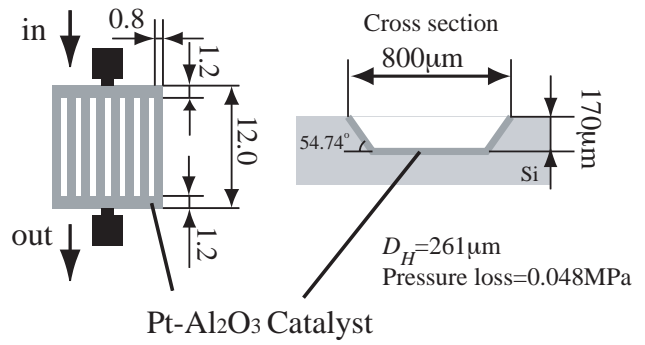


Figure 5 Schematic of micro catalytic combustor on Si substrate.

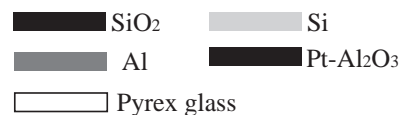
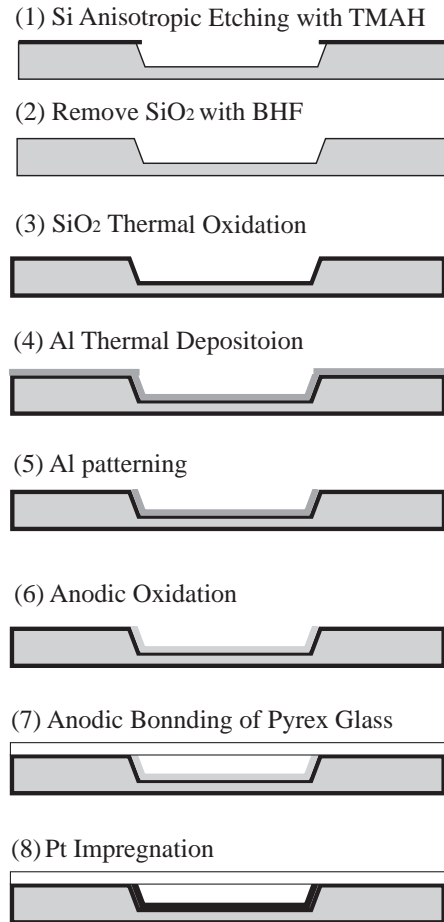


Figure 6 Fabrication process of micro combustor.

thickness of the aluminum is 5μm. In our preliminary experiment, polyimide tube is attached on the top of the ports using high-temperature glue. As shown in Fig. 8, preliminary experimental data gives 55% conversion for  $Q=10W$ , which is somewhat smaller reaction rate if compared with the tube combustor. It is conjectured that this is primary due to the thinner thickness of the alumina support.

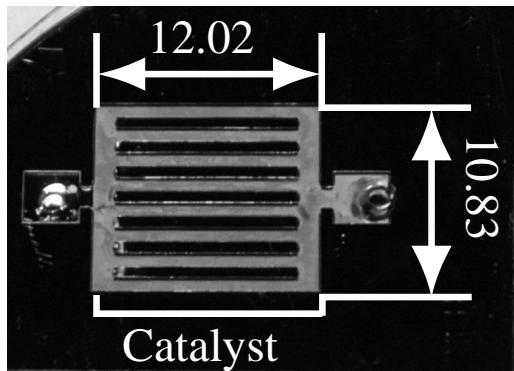


Figure 7 Si-based micro catalytic combustor.

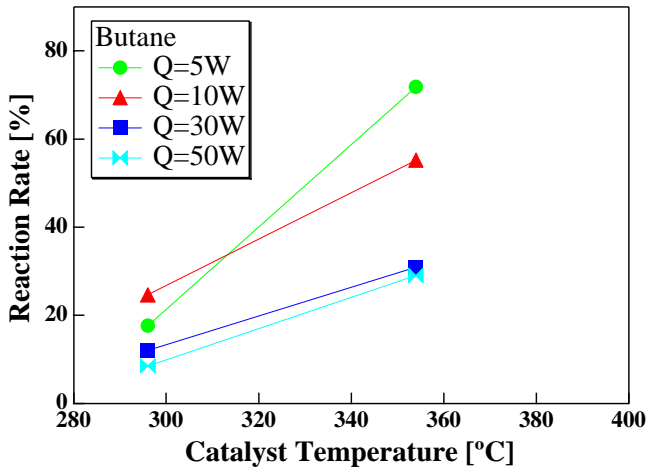


Figure 8 Reaction rate in Si-based micro catalytic combustor.

### CONCLUSIONS

Micro catalytic combustion of butane using an anodized alumina support is investigated. It is found in combustion experiments using 0.6mm ID tube that combustion starts at 250 °C, and a heat release rate up to 250MW/m<sup>3</sup> is achieved. A silicon-based catalytic combustor with embedded Pt/alumina catalyst layer is designed and its prototype is successfully fabricated using MEMS technologies. It is found in a preliminary experiment that the MEMS combustor also works reasonably well, but gives somewhat smaller reaction rate due to its thinner support layer.

### ACKNOWLEDGMENT

This work was supported through the Grant-in-Aid for Young Scientists A (No. 14702028) by the Ministry of Education, Science, Culture and Sports (MEXT).

### REFERENCES

[1] Freedonia Industry Study, World batteries, (2002).  
 [2] Epstein, A. H., Senturia, S. D., Al-Midani, O., Anathasuresh, G., Ayon, A., Breuer, K., Chen, K.-S., Ehrich, F. E., Esteve, E., Frechette, L., Gauba, G., Ghodssi, R., Groshenry, C., Jacobson, S., Kerrebrock, J. L., Lang, J. H.,

Lin, C.-C., London, A., Lopata, J., Mehra, A., Mur Miranda, J. O., Nagle, S., Orr, D. J., Piekos, E., Schmidt, M. A., Shirley, G., Spearing, S. M., Tan, C. S., Tzeng, Y.-S., and Waitz, I. A., "Micro-heat engines, gas turbines, and rocket engines - the MIT microengine project-," 28th AIAA Paper 97-1773, (1997), pp. 1-12.

[3] Fernandez-Pello, A. C., Pisano, A. P., Fu, K., Walther, D., Knobloch, A., Martinez, F., Senesky, M., Jones, D., Stoldt, C., and Heppner, J., "MEMS Rotary Engine Power System," Proc. Int. Workshop on Power MEMS 2002, Tsukuba, Japan, (2002), pp. 28-31.

[4] Palo, D. R., Holladay, J. D., Rozmiarek, R. T., Guzman-Leong, C. E., Wang, Y., Hu, J., Chin, Y.-H., Dagle, A., and Baker, E. G., "Development of a soldier-portable fuel cell power system Part I: A bread-board methanol fuel processor," J. Power Sources, 108, (2002), pp. 28-34.

[5] Schaevitz, S., Franz, A. J., Jensen, K. F., and Schmidt, M. A., "A combustion-based MEMS thermoelectric power generator," Proc. 11th Int. Conf. on Solid-State Sensors and Actuators, Munich, Germany, (2001), pp. 30-33.

[6] Fukui, T., Shiraiishi, T., Murakami, T., and Nakajima, N., "Study on High Specific Power Micro-Stirling Engine," JSME Int. J., Ser. B., 42, (1999), pp. 776-782.

[7] Sitzki, L., Borer, K., Schuster, E., and Ronney, P. D., "Combustion in microscale heat-recirculating burners," 3rd Asia-Pacific Conf. on Combustion, Seoul, (2001).

[8] Wang, X., Zhu, J., Bau, H., and Gorte, R. J., "Fabrication of micro-reactors using tape-casting methods," Catalysis Lett., 77, (2001), pp. 173-176.

[9] Arana, L. R., Schaevitz, S. B., Franz, A. J., Jensen, K. F., and Schmidt, M. A., "A microfabricated suspended-tube chemical reactor for fuel processing," Proc. IEEE Int. Conf. MEMS '02, Las Vegas, (2002), pp. 232-235.

[10] Spadaccini, C. M., Zhang, X., Cadou, C. P., Miki, N., and Waitz, I. A., "Preliminary development of a hydrocarbon-fueled catalytic micro-combustor," Sensors and Actuators, A, 103, (2003), pp. 219-224.

[11] Splinter, A., Sturmman, J., Bartels, O., and Benecke, W., "Micro membrane reactor: a flow-through membrane for gas pre-combustion," Sensors and Actuators, B 83, (2002), pp. 169-174.

[12] Sulka, G. D., Stroobants, S., Moshchalkov, V., Borghs, G., and Celis, J.-P., "Synthesis of well-ordered nanopores by anodizing aluminum foils in sulfuric acid," J. Electrochem. Soc., 149, (2002), D97-D103.

[13] Sungkono, I. E., Kameyama, H., and Koya, T., "Development of catalytic combustion technology of VOC materials by anodic oxidation catalyst," Appl. Surf. Sci., 121/122, (1997), pp. 425-428.